1971-09

Experiments with a simple hurricane-interacting ocean model

Corgnati, Leino Bartholomew, Jr.

Monterey, California; Naval Postgraduate School

EXPERIMENTS WITH A SIMPLE HURRICANE-INTERACTING OCEAN MODEL

Leino Bartholomew Corgnati

United States
Naval Postgraduate School

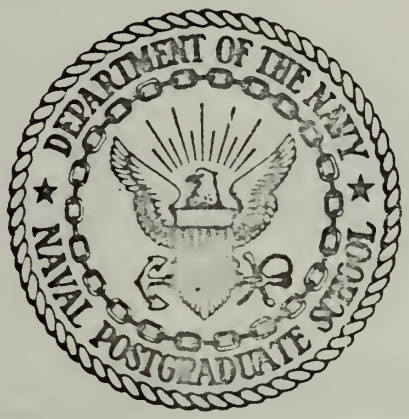

THESIS

EXPERIMENTS WITH A SIMPLE
HURRICANE-INTERACTING OCEAN MODEL

by

Leino Bartholomew Corgnati, Jr.

Thesis Advisor: R. L. Elsberry

September 1971

Experiments With A Simple Hurricane-Interacting Ocean Model

By

Leino Bartholomew Corgnati, Jr.
Lieutenant, United States Navy
B.S., United States Naval Academy, 1964

Submitted in partial fulfillment of the
requirements for the degree of

MASTER OF SCIENCE IN METEOROLOGY

from the

NAVAL POSTGRADUATE SCHOOL
September 1971

ABSTRACT

The equations developed by Riehl (1963) for a steady, symmetrical hurricane are used to specify a vortex over a fixed depth boundary layer, which interacts with a simple ocean model. Only vertical mixing in the surface layer is included in the oceanic portion of the model. Interaction of the atmosphere and the ocean occurs through the prediction of boundary layer parameters. Bulk aerodynamic equations are used to calculate the air-sea interaction. Comparison of the predicted boundary parameters with observed mature tropical storms shows good agreement for all variables except the specific humidity, which exceeds saturation. Two attempts to correct for this situation have shown that small changes in the surface moisture and temperature values strongly affect the maximum wind speed predicted. The proportion of the water vapor transported out of the top of the boundary layer without adding latent heat to the boundary layer appears to be an important factor in determining the intensity of a steady-state hurricane.

Although the ocean model is quite simple, realistic horizontal oceanic temperature profiles with respect to the hurricane center were obtained. However the magnitude of changes in oceanic heat content and the sea-surface temperatures were smaller than expected in actual hurricanes, since advection and upwelling effects were not included in the ocean model.

TABLE OF CONTENTS

I. INTRODUCTION 9

II. DISCUSSION OF THE MODEL 13

A. REVIEW OF RIEHL'S MODEL..... 13

1. Outflow Layer 13

2. Inflow Layer 14

3. The Steady State Value of V_θ 16

B. PREDICTION EQUATIONS 17

1. Atmospheric Prediction 17

2. Oceanic Prediction 21

C. INTERACTION BETWEEN THE ATMOSPHERIC AND OCEAN MODELS 22

D. INITIALIZATION OF SURFACE TEMPERATURES AND HUMIDITIES 23

III. ATMOSPHERIC MODEL PROFILES 28

IV. MODIFICATION OF THE MODEL 34

V. OCEANIC MODEL PROFILES 45

VI. CONCLUSION 51

BIBLIOGRAPHY 53

INITIAL DISTRIBUTION LIST 54

FORM DD 1473 55

LIST OF ILLUSTRATIONS

Figure		Page
1.	Hurricane mass circulation.....	15
2.	Polar coordinate system used.....	15
3.	Evolution of atmospheric temperature at the eye wall for two initialization procedures. (See text.) Equation solution refers to the simultaneous solution of Eqs. 23 and 24.....	27
4.	Same as Fig. 3 except for specific humidity at the eye wall.....	27
5.	Typical profile of the radial component of wind for the basic model beginning from initial maximum wind of 110 kts.....	29
6.	Same as Fig. 5 except for vertical motion in pressure coordinates.....	29
7.	Same as Fig. 5 except for atmospheric temperature. Right hand scale represents the difference between oceanic and atmospheric temperature.....	31
8.	Same as Fig. 5 except for specific humidity	31
9.	Same as Fig. 5 except for accumulated precipitation from large scale moisture flux after one hour.....	32
10.	Same as Fig. 5 except for sensible heat (Qs) and latent heat (Qe) exchange for the surface. Ocean temperature is fixed at 30C.....	32
11.	Evolution of specific humidity at the eye wall for the same experiment as described in Fig. 5....	35
12.	Evolution of relative humidity at the eye wall for the same experiment as described in Fig. 5....	35
13.	Evolution of atmospheric temperature (upper diagram) and specific humidity (lower diagram) with time for experiment with and without Robinson's C_D reduction.....	37

14. Convective moisture mechanism without Ta adjustment. Note that a loss of moisture through top of boundary layer occurs with ascent in clouds and compensating descent in the environment..... 39

15. Convective moisture mechanism with Ta adjustment. Note warming from the release of latent heat occurring in the boundary layer.... 39

16. Specific humidity with varying amounts of convective moisture reduction (fraction of 1% removal) for a critical relative humidity of 95%. (See text.)..... 40

17. Specific humidity with varying relative humidity criteria for a convective moisture reduction of .75 of 1%. (See text.)..... 40

18. Maximum tangential wind speed (upper diagram) and specific humidity (lower diagram) for various initial v_{θ_i} values with a convective mechanism without a temperature adjustment..... 41

19. Maximum tangential wind speed (upper diagram) and specific humidity (lower diagram) for various initial v_{θ_i} values with a convective mechanism with a temperature adjustment..... 43

20. Hurricane heat potential loss for varying daily observations for a convective mechanism without a temperature adjustment..... 46

21. Sea-surface temperature loss for varying daily observations for a convective mechanism without a temperature adjustment..... 46

22. Same as Fig. 20 except for convective mechanism with a temperature adjustment..... 47

23. Same as Fig. 21 except for convective mechanism with a temperature adjustment..... 47

24. Comparison of maximum tangential wind speed with sea-surface temperature fixed (Tw fixed) and sea-surface temperature allowed to vary (Tw free) for the model incorporating a convective mechanism with and without temperature adjustment..... 50

LIST OF SYMBOLS

Cp	Specific heat of air at constant pressure.
C_D	Drag coefficient.
E	Energy exchange potential.
e_s	Saturation vapor pressure.
f	Coriolis parameter.
HHP	Hurricane heat potential.
L	Latent heat of vaporization of water.
P	Pressure.
Qa	Specific humidity at Ta.
Qe	Latent heat release rate.
Qs	Sensible heat transfer.
Qw	Saturated specific humidity at Tw.
r	Radial distance from center of hurricane.
rh	Radius at which v = 25 m/sec.
ri	Radius of maximum tangential wind.
r_o	Radius from center of hurricane where tangential wind component is equal to zero in the outflow layer.
$\overline{T}$	Mean temperature of ocean layer.
Ta	Atmospheric temperature.
Tae	Pseudo-equivalent temperature.
Tw	Sea surface temperature.
u	Velocity component in x direction
v	Velocity component in y direction.
V_r	Radial wind component.

V_θ	Tangential wind component.
V_{θ_h}	Tangential wind component set at 25 m/sec.
V_{θ_i}	Maximum tangential wind component.
ΔP	Thickness of boundary layer.
α	Inflow angle.
θ	Angular measurement.
θ	Potential temperature.
θ_e	Equivalent potential temperature.
θ_{ei}	Equivalent potential temperature at the eye wall.
θ_{e_o}	Equivalent potential temperature at r_o.
ρ_s	Density of air.
τ	Frictional surface stress.
ω	Velocity component in vertical direction.

ACKNOWLEDGEMENT

The author wishes to express his sincere gratitude to Dr. R. Elsberry whose guidance, encouragement, and store of information were essential to this work.

I. INTRODUCTION

Observational and numerical investigations of tropical hurricanes have been made by many tropical meteorologists. Dynamical and structural features of mature three-dimensional tropical storms are not completely clear but much has been learned through the use of steady-state axisymmetric hurricane models. Malkus and Riehl (1960) examined the dynamics and energy transformations in such a steady-state hurricane.

Investigation of inflow trajectories, shown in Figure 1, gave insight to the oceanic heat source necessary for the maintenance of a steady-state storm. The dynamic model of the inflow layer developed useful relations between wind speed, pressure gradient, surface shearing stress, mass flow and convergence.

In a more recent work, Riehl (1963) examined some relations between wind and the thermal structure of the steady-state hurricane. The steady-state hurricane is defined as one in which a balance exists between the heat source and momentum sink at the air-sea interface. In terms of a bulk aerodynamic estimate of these processes, the heat source depends linearly on wind speed while momentum sink depends on the square of the wind speed. A steady hurricane model was developed to compare with observed storms. A two-layer model was considered with conservation of absolute angular momentum assumed in the outflow layer, shown in Figure 1, and conservation of potential vorticity assumed in the inflow. With

these assumptions the momentum transport at the air-sea interface can be specified, and thus the radial profile of the tangential wind component. By assuming the kinetic energy necessary to drive a hurricane is provided by the oceanic heat source, Riehl estimated the heat source required for a given wind field to exist in steady state.

The purpose of this study is to utilize the steady-state hurricane model proposed by Riehl in experiments with an interacting ocean model. Air-sea exchanges beneath the tropical storm will be examined for a constant depth surface boundary layer interacting with the ocean surface.

Several numerical simulations of hurricane development have been made with complicated multi-level models. These models, which require very short time steps, included some interaction with the ocean. The scope of the study is to model only the boundary layer beneath a specified vortex. The Riehl model is, therefore, used as a diagnostic model assuming that it applies at each time step. The steady-state vortex above the boundary layer is defined by Riehl's model, which is specified by air-sea interaction.

Specification of the boundary layers under the circulation provides an opportunity to study the changes in the ocean as well as the vortex. An essential assumption carried over from Riehl was a steady, symmetrical vortex which in early experiments, is stationary. Leslie and Smith (1970) point out that the importance of the surface boundary layer on the dynamics of a hurricane is due to the meridional

circulation of the vortex, providing a strong coupling between the azimuthal and vertical velocity fields. However this study will use the simple boundary layer of Riehl.

Several investigations have shown that areas of low sea-surface temperatures occur in the wake of hurricanes. Jordan (1964) analyzed sea-surface temperature for the months of typhoon seasons and reported marked cooling of the ocean surface with passage of the hurricane. Leipper (1967) analyzed oceanic temperature for hurricane Hilda of 1964. In the latter study, comparison of pre-storm merchant ship reports and post-storm data, gathered by a planned cruise of the area in the Gulf of Mexico where Hilda passed, indicated significant cooling in the surface layer during the passage. Jordan suggested that cooling of the sea-surface temperature was due, in part, to upwelling of cooler water or vertical mixing caused by the winds. Jordan concluded that mixing was the more important factor. However, other authors such as Fisher (1958) have considered upwelling to be the most important. Leipper (1967) stated that in addition to upwelling of cooler waters and vertical mixing of the surface layer, horizontal advection of surface waters and the thermal transfer of energy from the ocean to the atmosphere are important factors in determining the observed oceanic thermal structures. Leipper concluded that the dominant process in the observed cooling is the Ekman suction resulting from wind mixing and that upwelling is the next most important. A theoretical two-layer ocean model developed by O'Brien and

Reid (1967) to simulate circulation beneath a hurricane verified that upwelling was an important factor.

In this research the oceanic model is an elementary attempt to simulate the ocean temperature field resulting from vertical mixing due to the air-sea exchange. Eventual refinements of the ocean model may include upwelling of cooler water and oceanic advection, and also movement of the hurricane over the ocean will allow prediction of the oceanic effects. Volgenau (1970) has incorporated the oceanic effect in terms of the hurricane heat potential (HHP) which is defined as the excess of heat content over that of water at 26C.

Those specific quantities examined in this study are the temperature and moisture fields of both the atmosphere and the ocean, the effects of the atmosphere upon the oceanic fields and vice-versa. Also the effect of varying initial maximum wind speeds will be examined. Eventual study will include the effects of a varying drag coefficient in the boundary layer. In general, this study is an attempt to create an interacting model of a hurricane boundary layer and a simple ocean model, which may be developed into more detailed descriptions of the effects of sea-air interaction in hurricanes.

II. DISCUSSION OF THE MODEL

This study is an experiment with the steady-state, symmetrical hurricane as described by Riehl (1963); therefore this discussion will follow relevant development in his paper.

A symmetric, 17x17 rectangular grid is used in Cartesian coordinates with 15 nautical mile spacing. The center of the hurricane coincides with the center of the grid and the eye wall is linked to the first grid point outbound along a diagonal. Cartesian coordinates are used to link the symmetrical hurricane to the model of an ocean within a rectangular region. In the initial experiments the hurricane is stationary, but eventually the hurricane will be moved with respect to the ocean model in a Cartesian coordinate system. Transformation from the arbitrary Cartesian grid to polar coordinates centered on the eye of the hurricane is part of the procedure. (See Fig. 2)

A. REVIEW OF RIEHL'S MODEL

1. Outflow Layer

The initial parameters include the maximum tangential wind component, $v_{\theta i}$, the radius of maximum wind, r_i, along with the latitude of the storm. Riehl and Malkus (1961) have shown that conservation of absolute angular momentum is a reasonable first approximation in the outflow layer. (See Fig. 1) This constraint leads to the following

expression for computing r_o, the radius where $v_\theta = 0$,

$$r_o = (2 v_{\theta i} r_i / f)^{1/2}, \qquad (1)$$

where f is the coriolis parameter. It is noted that by specifying the eye wall or maximum wind at a diagonal grid point, r_o becomes a function of the grid spacing. Variables which are dependent on radius only are computed along a diagonal. Those variables include pressure, vertical motion, temperature and moisture advection, and large scale moisture flux.

2. Inflow Layer

Conservation of potential vorticity in the inflow layer was also demonstrated by Riehl and Malkus (1961). Matching the outflow and inflow layer at the eye wall leads to the relationship,

$$v_\theta r^{1/2} = \text{CONST}, \qquad (2)$$

which is a good approximation to v_θ-r profiles found in mature hurricanes (see examples in Riehl, 1963). Inside the eye wall, solid body rotation is assumed to determine v_θ. Thus given $v_{\theta i}$ and r_i, the tangential component of the wind can be determined from Eq. (2) at any radius. In particular the tangential wind at the radius r_o is used in the calculation of the initial radial component of the wind.

Integration of the momentum equation over a shallow inflow layer of thickness Δp where potential vorticity is assumed to be conserved, results in the following expression

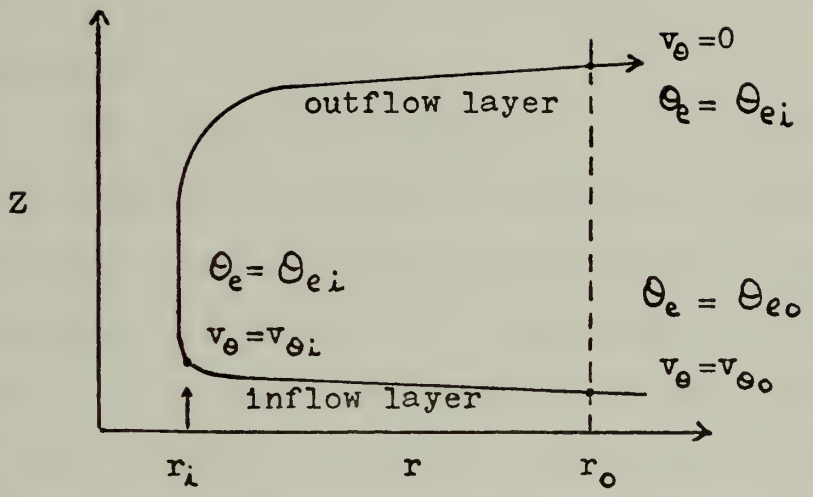

Illustrating hurricane mass circulation v_θ is tangential wind component, θ_e is equivalent potential temperature, r is radius

Figure 1

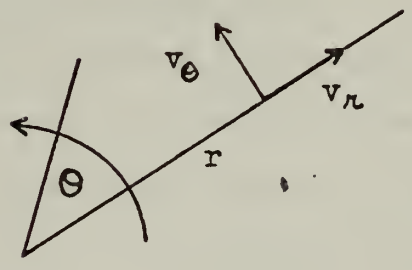

Illustrating polar coordinate system used v_θ is tangential wind component, v_r is radial wind component, r is radius, θ is angular measurement

Figure 2

for the radial wind component,

$$v_r = g/\Delta P \; r_0 v_{\theta_0}^2 \Big/ v_{\theta_0} \left(\frac{r_0}{r}\right)^{1/2} + 2fr, \qquad (3)$$

where g is the acceleration of gravity and ΔP is the inflow thickness set at 100 mb.

The tangential component at the surface (v_{θ_0}) must also be specified to define a complete surface wind for calculation of the air-sea boundary fluxes. Therefore v_{θ_0} was assumed to be 0.7 of the wind speed at the top of the boundary layer, which was specified by Eq. (2). The use of this coefficient is equivalent to specifying an effective drag coefficient based on the tangential component at the top of the boundary layer. Choosing a value of 0.7 reduces the drag coefficient (C_D) by a factor of 0.49 for momentum exchange, and by 0.7 for the heat and moisture exchanges. As noted in the introduction the heat source depends linearly on wind speed while momentum sink depends on the square of the wind speed.

3. The Steady State Value of V

Riehl proposed that a particular relation exists between the heat source and momentum sink in the interior of hurricanes, if a steady state velocity field is observed. This proposal leads to the following expression for the maximum wind speed,

$$v_{\theta i}^2 \, (m/sec) = 10^2 E \left[\ln \frac{r_h}{r_i} + \frac{4 f r_h}{3 v_{\theta h}} \right] \qquad (4)$$

which satisfies both the tangential distribution from

momentum and from heat source considerations, where r_h is the point where v_{θ_h}=25 m/sec. as chosen by Riehl. An energy exchange potential parameter, E, is defined as,

$$E = (T_w - T_a) + L/C_p (Q_w - Q_a) \tag{5}$$

where Tw and Qw are the temperature (C) and the saturated specific humidity (gm/kgm) at the sea surface and Ta and Qa are the temperature and specific humidity of the atmosphere in the boundary layer. L represents the latent heat of vaporization (597.3 cal/gmw) and Cp is specific heat constant for (.24 cal/gm deg).

B. PREDICTION EQUATIONS

1. Atmospheric Prediction

In the atmosphere the predicted variables are the potential temperature and the specific humidity above the sea surface. These two parameters, along with pressure, determine the equivalent potential temperature θ_e. Riehl (1963) has shown that θ_e is one factor in determining the maximum wind.

The thermodynamic equation is used in the following form,

$$\frac{\partial \theta}{\partial t} = - \left[\frac{\partial v_\theta \theta}{r \partial \theta} + \frac{\partial v_r r \theta}{r \partial r} + \frac{\partial \omega \theta}{\partial P} \right] + Q_s \tag{6}$$

where θ is the potential temperature (K), ω is the vertical motion (mb/hr), P is pressure (mb) and Qs is sensible heat transfer. The first term on the right hand side of Eq. (6) is neglected due to symmetry. Potential temperature is

assumed to be constant in the boundary layer and thus could be created from the air temperature (Ta) field knowing the surface pressure. The effect of expansion cooling is included by using potential temperature in the thermodynamic equation.

Moisture changes were determined in similar fashion using,

$$\frac{\partial Q_a}{\partial t} = -\left[\frac{\partial V_\theta Q_a}{r\partial\theta} + \frac{\partial V_r r Q_a}{r\partial r} + \frac{\partial \omega Q_a}{\partial P}\right] + Q_e, \qquad (7)$$

where Qa is the specific humidity (gm/kgm) and Qe is the latent heat transfer. The first term on the right hand side is neglected because of symmetry.

Because the ocean model is in Cartesian coordinates, surface exchange values are computed in rectangular coordinates. The transfer of sensible heat per unit volume is computed with the bulk transport equation in the form,

$$Q_s/C_p = \rho_s C_D (T_W - T_A)\sqrt{u^2 + v^2}, \qquad (8)$$

in units of cal/sq cm sec where Cp is specific heat, ρ_s is the atmospheric density above the sea surface, Tw is the temperature of the ocean, Ta is the atmospheric temperature, and $\sqrt{u^2+v^2}$ represents the total wind speed. Latent heat transfer or the rate of moisture input per unit volume is calculated by,

$$Q_e/L = \rho_s C_D (Q_w - Q_a)\sqrt{u^2+v^2}, \qquad (9)$$

in units of cal/sq cm sec where L is the latent heat of

vaporization, Qw is the specific humidity at the temperature of the ocean surface (Tw) and Qa is the specific humidity of the atmosphere. The Bowen ratio is defined as the ratio of sensible heat to latent heat exchange and is an indication of the relative importance of these two mechanisms of energy transfer from the ocean to the atmosphere.

For use in Eq. (8) and (9), the wind is delineated into u and v Cartesian components. Cartesian components are transformed from the radial and tangential components of the wind as follows,

$$u = V_r \cos\theta - V_\theta \sin\theta$$
$$v = V_r \sin\theta + V_\theta \cos\theta \quad , \tag{10}$$

where the angle θ increases in a counter-clockwise direction from the x-axis so that u is positive for westerly winds and v is positive for southerly winds.

The equation of motion in polar coordinates, neglecting lateral friction, was used to determine the radial component of the wind, v , which was in balance with the new tangential wind component obtained from the following equation,

$$\frac{dV_\theta}{dt} + \frac{V_\theta V_r}{r} + fV_r = -\frac{1}{\rho}\frac{\partial P}{r\partial\theta} \quad \frac{1}{\rho}\frac{\partial \tau}{\partial z} \quad , \tag{11}$$

In pressure coordinates, assuming a steady state, Eq. (11) yields,

$$V_r = \frac{-g \frac{\partial \tau}{\partial P}}{f + \frac{\partial V_\theta}{\partial r} + \frac{V_\theta}{r}} \quad , \tag{12}$$

where τ is the wind stress, $\partial P / \partial \theta$ is zero due symmetry of the storm, $\omega \frac{\partial v_\theta}{\partial P}$ is zero because ω is zero at the surface and $\frac{\partial v_\theta}{\partial P}$ is assumed zero at the top of the boundary layer. A boundary layer factor of 0.7 was incorporated to account for the vertical profile, as was described in the inflow layer section, II A. The surface stress is defined to be proportional to the square of the surface wind,

$$\tau_{\theta s} = C_D \rho_s v_{\theta s}^2 / \cos \alpha , \qquad (13)$$

where α is the inflow angle measured relative to isobars. The stress is assumed to be zero at the top of the boundary layer.

Computations of vertical motion and advection in Cartesian coordinates did not prove to be successful. This was because any values such as vertical motion or the advection quantities, which involve x and y derivatives were not symmetrical with respect to the diagonals. Therefore, asymmetries resulted in the temperature and moisture fields and prevented long period predictions. Transforming to a polar coordinate system for the computation of vertical motion and the advection quantities conserved the symmetry of the initial fields. Also, for asymmetric temperature and moisture fields, a small error is introduced by the neglection of the azimuthal advection. Due to the large tangential velocities in a hurricane, various properties tend to be symmetric with respect to the center and omitting the azimuthal advection introduces a much smaller error than the use of Cartesian coordinates.

Vertical motion at the top of the boundary layer was computed from the continuity equation, in polar coordinates,

$$\frac{\partial V_\theta}{r\,\partial\theta} + \frac{\partial r V_r}{r\,\partial r} + \frac{\partial \omega}{\partial P} = 0 \,, \qquad (14)$$

where the change of the tangential wind with respect to angular change is zero in a symmetric storm. Vertical motion at the surface is assumed to be zero and the boundary layer is chosen to be 100 mb thick as an approximation to the first kilometer of a tropical atmosphere.

2. Oceanic Prediction

Predicted variables in the oceanic portion of the model are the sea-surface temperature (Tw) and the saturated specific humidity (Qw) at temperature Tw. A crude approximation of the oceanic energy loss centers on the concept of hurricane heat potential, HHP, defined by Volgenau (1970) as the excess of heat content over that of water at 26 C. A temperature profile as shown

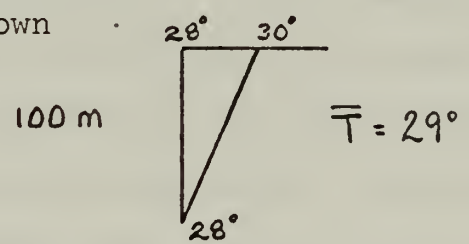

defines a hurricane heat potential of 3×10^4 cal/sq cm by,

$$HHP = C_p (\bar{T} - 26) \times \text{DEPTH} \,, \qquad (15)$$

where $\bar{T}$ is the mean temperature of the chosen ocean layer with a depth of 100 meters. The loss of energy by the ocean or the change in heat potential is equal to the sensible and latent transfer of energy during each time step,

that is,

$$\Delta HHP = \Delta t \times 3600.0 \times (Q_s + Q_e) , \qquad (16)$$

where Δt is the prescribed time step. After a time step the reduced magnitude of heat potential corresponds to a new mean temperature in the upper layer of the ocean and thus a sea-surface temperature can be calculated. This scheme accounts for sensible heating and evaporation but neglects radiation gains, horizontal divergence or upwelling. Since the saturation specific humidity field is computed from the Clapeyron equation, the evaporation from the sea surface is decreased as the surface temperature is decreased.

C. INTERACTION BETWEEN THE ATMOSPHERIC AND OCEAN MODELS

In the atmospheric model the maximum wind speed determined by the heat source is a function of the energy exchange potential, E, as given by Eq. (4). A new mean value of $\bar{E}$ was calculated after each time step using the newly predicted atmospheric and oceanic parameters. However the ocean is effectively an infinite heat source and the result of this approach was to bring the atmosphere into equilibrium with the ocean, that is, E tended to zero. Consequently the maximum wind speed predicted from Eq. (4) also decreased to zero although very warm and moist air was available in the atmospheric boundary layer.

In a second approach, the maximum wind speed was calculated from the equivalent potential temperature at the eye

wall as follows,

$$v_{\theta i}\,(m/sec) = 14.1\,(\theta_{ei} - \theta_{e_o})^{1/2}, \qquad (17)$$

where θ_{e_o} is set at 350 K. The tangential wind component was computed at other grid points by the v_θ-r relationship as given by Eq. (2).

D. INITIALIZATION OF SURFACE TEMPERATURES AND HUMIDITIES

Integration of the hydrostatic equation for typical values of θ_e in a hurricane produces a relation,

$$P' = -2.56\,\theta_e', \qquad (18)$$

where P' is the pressure departure from 1005 mb and θ_e' is the equivalent potential temperature departure from 350 K. This expression specifies eye wall pressure variation caused by the oceanic heat source. With the use of Eq. (17) and (18), the pressure and equivalent potential temperature at the eye wall may be specified for a given maximum wind speed. The pressure distribution along each diagonal was then computed from the gradient wind equation. The pressure at intermediate points throughout the symmetric field was determined by linear interpolation using pressure at the eye wall and the distribution of v_θ with radius.

Initialization of the temperature and moisture fields both in the boundary layer and at the ocean surface are important parts of this model. In the initial experiments the sea-surface temperature, Tw, was initialized at a constant value of 30 C throughout the grid. The available

moisture at the ocean surface, Qw, was calculated from the integrated form of Clapeyron's equation for the saturation vapor pressure over water,

$$\text{LN}\frac{e_s}{6.105} = 25\,\frac{T-273}{T} - 5.2\,\text{LN}\frac{T}{273}, \qquad (19)$$

where e_s is the saturation vapor pressure. Assuming the air in contact with the water is saturated, specific humidity was calculated from,

$$\gamma_s = \frac{.622\,e_s}{P - .373\,e_s}, \qquad (20)$$

in units of gm/kgm.

Two different methods were used for initialization of the air temperature and moisture fields within the boundary layer. One approach was to specify the initial values of the air temperature, Ta, and the specific humidity, Qa, in terms of the equivalent potential temperature at the eye wall which is related to the maximum tangential wind in Eq. (17). Specification of initial parameters at the eye wall from equivalent potential temperature is consistent with the scheme used in predicting the new maximum wind speed. This method involved the solution of two simultaneous equations defining E and the pseudo-equivalent temperature. These equations were,

$$Qa = Qw - C_P/L\left[E - (T_W - Ta)\right], \qquad (21)$$

and,

$$Qa = Ta\,\frac{C_P}{L}\,\text{LN}\,\frac{Tae}{Ta}, \qquad (22)$$

where Tae is the pseudo-equivalent temperature. Following Riehl, it was assumed that E may be treated as constant over the inner region of a hurricane and the equivalent potential temperature difference between the eye wall and the outer regions of the storm is constant over the boundary layer depth Δz. Thus the expression for the effect of the total heat source in increasing the equivalent potential temperature is,

$$\theta_{ei} - \theta_{eh} = \frac{C_D}{\Delta z} E \int v_\theta \, dt, \qquad (23)$$

Effectively this expression implies bulk aerodynamic transfer of heat and moisture in a fixed boundary layer. The sensible and latent heat transfer where $r < r_h$ is crucial in determining the increased equivalent potential temperature required to generate hurricane force winds. The value of E was computed from Eq. (4). The adiabatic equivalent temperature is related to the equivalent potential temperature by,

$$\theta_e = T_{ae} \left(\frac{1000}{P}\right)^{0.286}. \qquad (24)$$

By specifying the initial state from the equivalent potential temperature at the eye wall, the effect of expansion cooling and sensible heat source at the surface are taken into account. Riehl suggested that θ_e must rise above 350-352K to allow deep convection which warms the column and lowers the central pressure to values which can sustain hurricane force winds.

Solution of Eqs. (23) and (24) gives an initial value of surface temperature and moisture at the eye wall.

Therefore expression Eq. (17) relating $v_{\theta i}$ to θ_{ei} applies only at the eye wall unless these values are specified elsewhere. To initialize the remainder of the Ta and Qa values it was assumed that the relative humidity varied linearly between the value determined at the eye wall and a value at the outer radius. The latter value was selected to be typical of undisturbed tropical air. For the remaining grid points simultaneous solution of the energy exchange potential, E, equation and the Clapeyron equation including the specified relative humidity was used to determine the initial state.

The present experiment has shown that a second approach may be as effective as the previous solution of simultaneous equations. By initializing the atmospheric temperature at an arbitrary value, say equal to the oceanic value, while the moisture was made consistent with the maximum wind speed through the equivalent potential temperature, it was found that the model came into balance with a steady-state hurricane after 10 hours. Comparison of the temperature and humidity fields produced by both approaches shown in Fig. 3 and 4, demonstrates this favorable result.

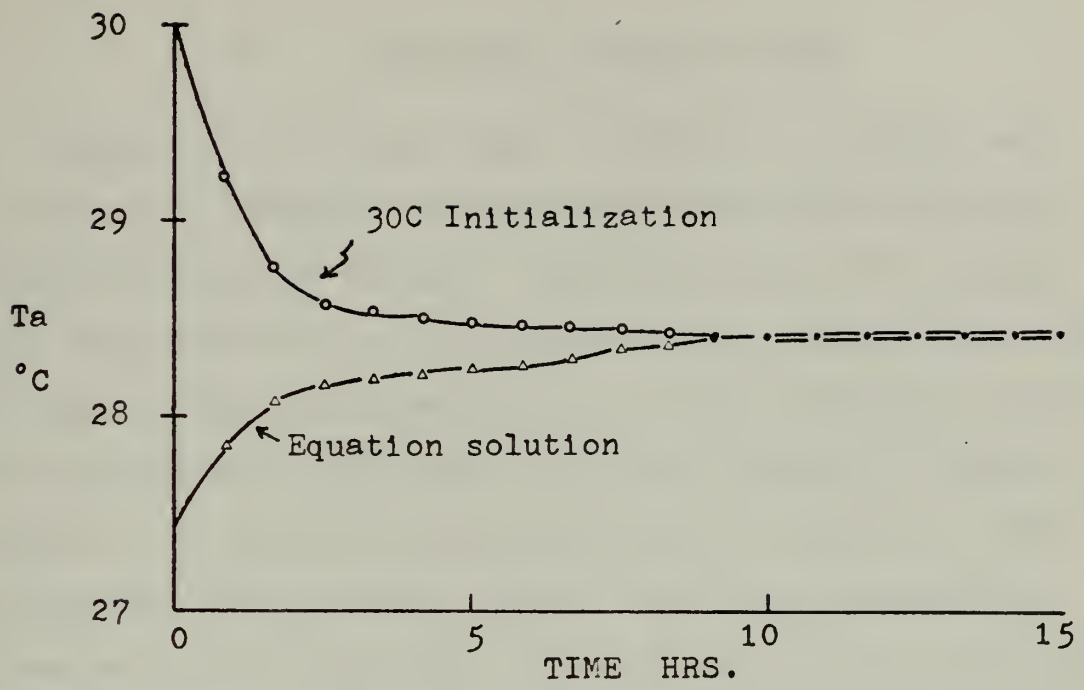

Evolution of atmospheric temperature at the eye wall for two initialization procedures. (See text.) Equation solution refers to the simultaneous solution of Eqs. 23 and 24.

Figure 3

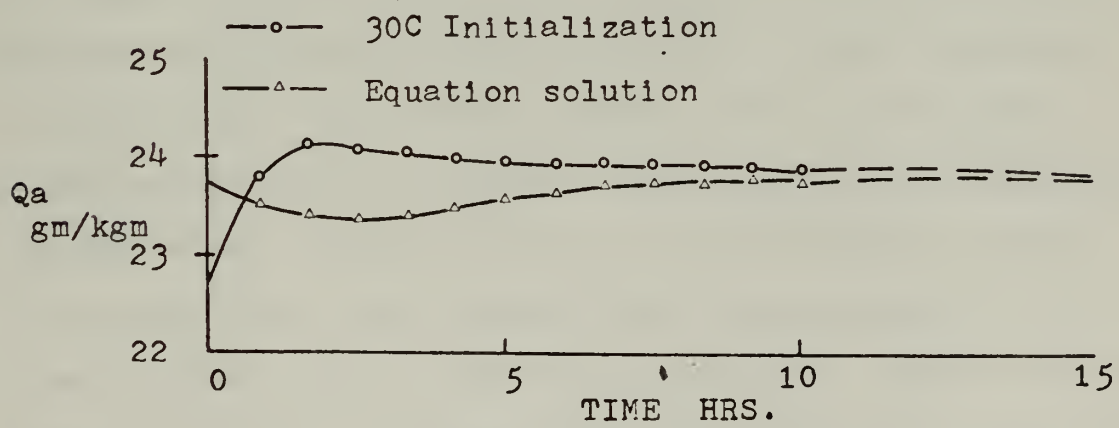

Same as Fig. 3 except for specific humidity at the eye wall.

Figure 4

III. ATMOSPHERIC MODEL PROFILES

Results of the basic model described in earlier sections may be compared with the observed surface structure of mature tropical storms. Specifications of the tangential wind profile, v_θ , according to Eq. (2) has been shown by Riehl (1963) to be realistic, yet the remaining variables of the predicted hurricane need to be verified. Observations of the surface characteristics of a hurricane have been summarized by Riehl (1954). For these comparison experiments the sea-surface temperature, Tw, was held fixed to model the steady-state atmospheric circulation.

The effect of the surface stress is to develop a cross-isobaric flow, the radial component of the wind (v_r), shown in Figure 5. The radial wind component increases toward the eye wall, with a maximum value of v_r which compares favorably with the velocity profile for a steady-state hurricane described by Riehl. Vertical motion is determined by the radial gradient of r v_r in an axisymmetric storm. All values of ω were negative with the strongest ascent concentrated near the center of the storm. Figure 6 illustrates the area of strong upward vertical motion resulting from the inflow near the eyewall. Note that no strong radial inflow bands, which would represent the satellite-observed cloud formations spiralling toward the hurricane center, can exist in the axisymmetric vortex.

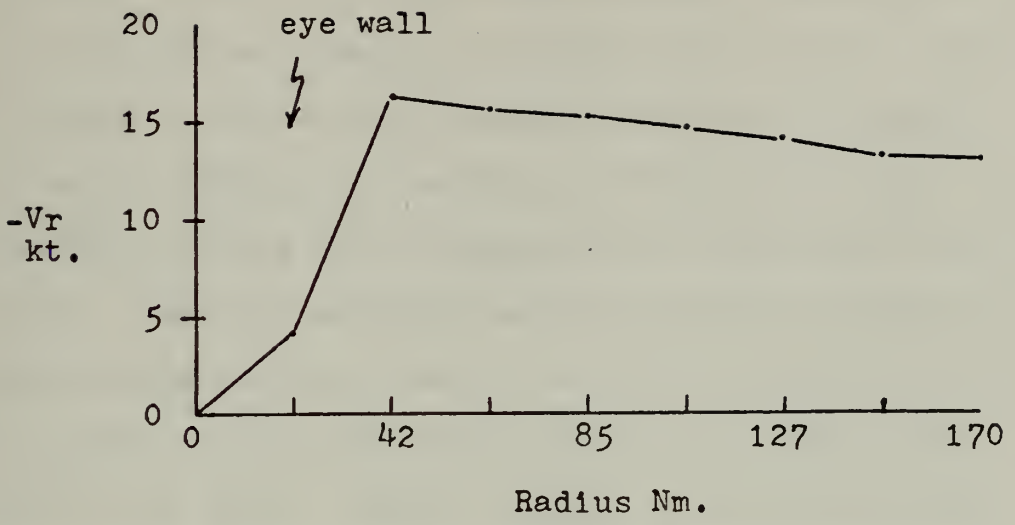

Typical profile of the radial component of wind for the basic model beginning from initial maximum wind of 110 kts.

Figure 5

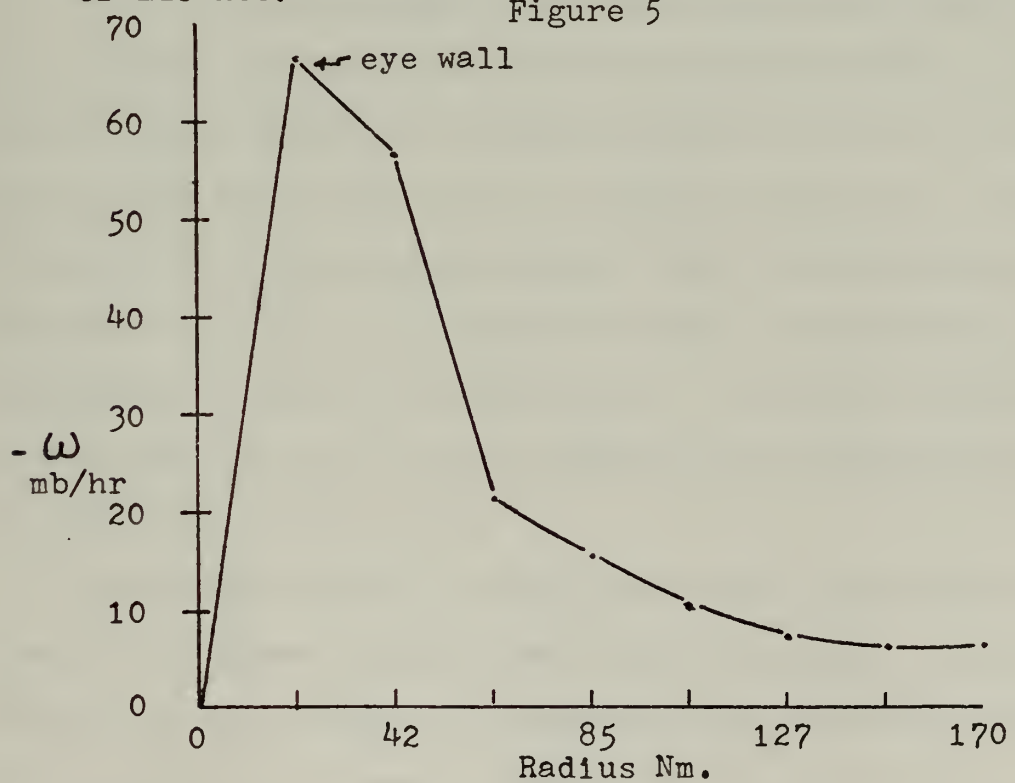

Same as Fig. 5 except for vertical motion in pressure coordinates.

Figure 6

Although potential temperature of the surface air increases along the inflow trajectories, the surface temperature decreases toward the storm center until a balance of expansion cooling and sensible heating is reached. The expected temperature pattern is verified by Fig. 7 with the maximum cooling of the surface air occurring at the eye wall. Specific humidity may be expected to increase along the inflow trajectories as the air in contact with the ocean acquires moisture through evaporation, which should increase with wind speed. Figure 8 shows a slight increase of moisture content predicted as the air moves inward.

It has been observed that precipitation in hurricanes is strongly concentrated near the inner core of a storm. Riehl (1954) notes the average rainfall rate at a fixed point will be on the order of 15-20 cm per day. For comparison the large scale moisture flux due to vertical motion through the top of the boundary layer was converted to an equivalent depth of precipitation. The model predicts only 3-4 cm per day, but Fig. 9 verifies the concentration of rainfall at the eye wall.

The surface layer air acquires both latent and sensible heat as it moves inward toward lower pressure. These results show that the transfer of sensible heat from the ocean to the atmosphere is small compared to the latent heat transfer. In the initial state the air temperature, Ta, is approximately equal to the sea-surface temperature, Tw, and the atmospheric specific humidity, Qa, is small compared to the

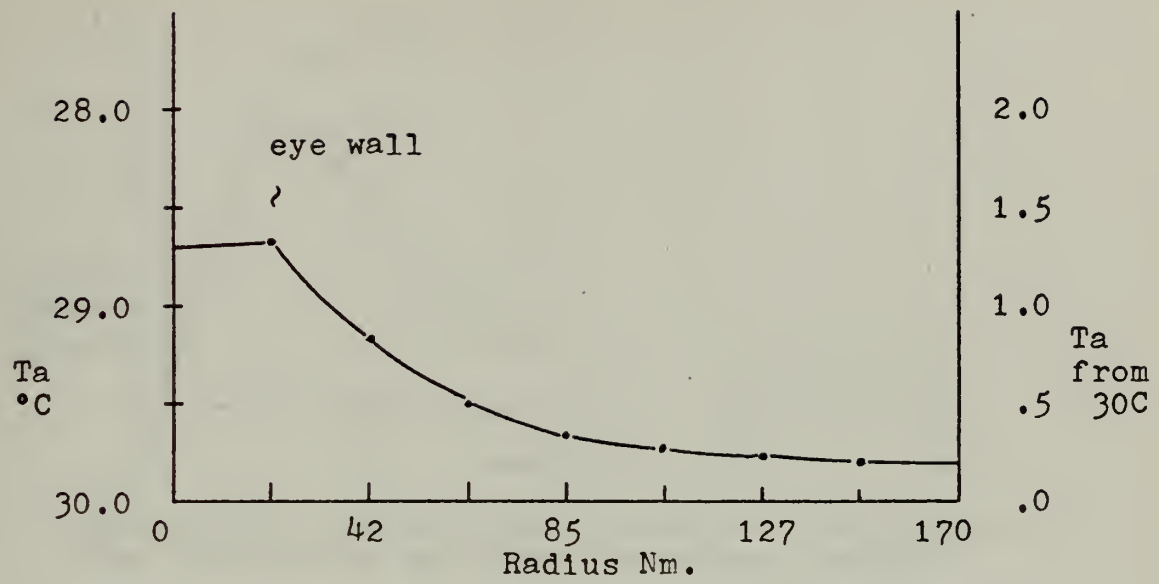

Same as Fig. 5 except for atmospheric temperature. Right hand scale represents the difference between oceanic and atmospheric temperature.

Figure 7

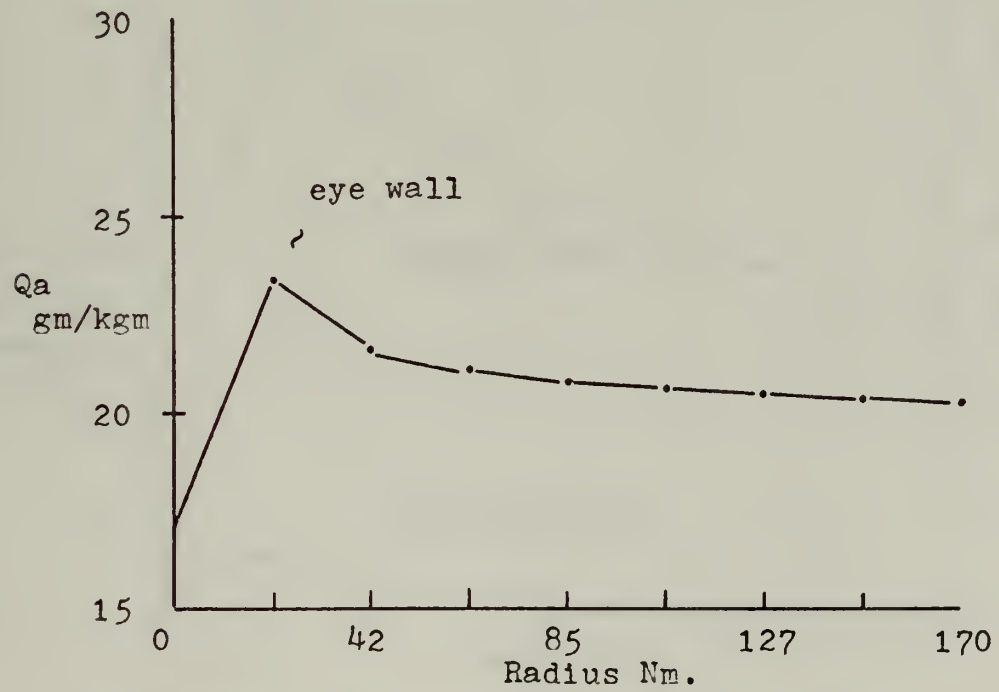

Same as Fig. 5 except for specific humidity.

Figure 8

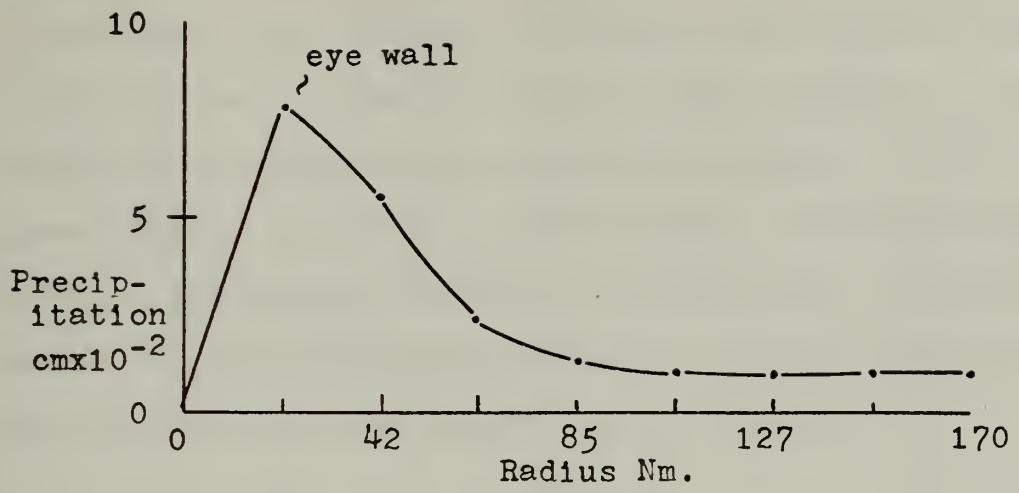

Same as Fig. 5 except for accumulated precipitation from large scale moisture flux after one hour.

Figure 9

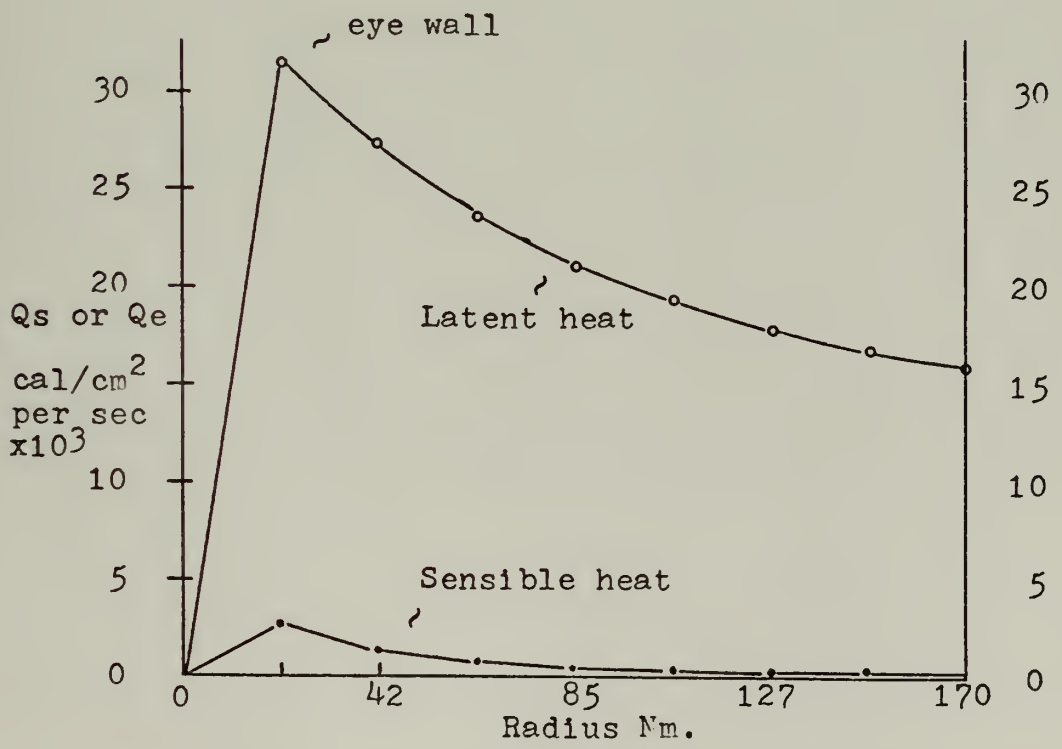

Same as Fig. 5 except for sensible heat (Qs) and latent heat (Qe) exchange for the surface. Ocean temperature is fixed at 30C.

Figure 10

saturation specific humidity at the ocean interface. Therefore latent heat transfer is larger than sensible heating. Figure 10 is a comparison of the heat transfer. The large addition of moisture due to evaporation may either be precipitated or stored in the column. The large precipitation at the eyewall is due to the fact that the moisture which is not precipitated along the radial inflow trajectory will be carried inward to the eye wall.

IV. MODIFICATION OF THE MODEL

An encouraging aspect of the initial experiments was obtaining the expected atmospheric horizontal temperature profile. However, prediction of moisture content represented a major shortcoming of the initial model. That is, the advection scheme plus the sensible heat exchange produced the expected temperature profile, but advection plus evaporation produced an excessive increase in moisture in the boundary layer. As shown in Fig. 12, surface relative humidity values at the eye wall exceeded saturated conditions after short time periods. Either the moisture transport due to vertical motion in Eq. (7) was not removing enough moisture from the boundary layer, or the evaporation from the sea was too large.

A possible explanation may be that the surface exchange of moisture was overestimated. Robinson (1966) reports that the drag coefficient, C_D, for the sensible and latent heat exchange at high wind speeds is less than the drag coefficient for momentum exchange by a factor of one-third. In the momentum exchange at the sea surface the pressure forces dominate over molecular processes at the interface. However near the air-sea interface molecular processes determine the rate of transport of heat and water vapor. Thus the transfer coefficient for momentum may differ from that for sensible heat and moisture exchanges which are

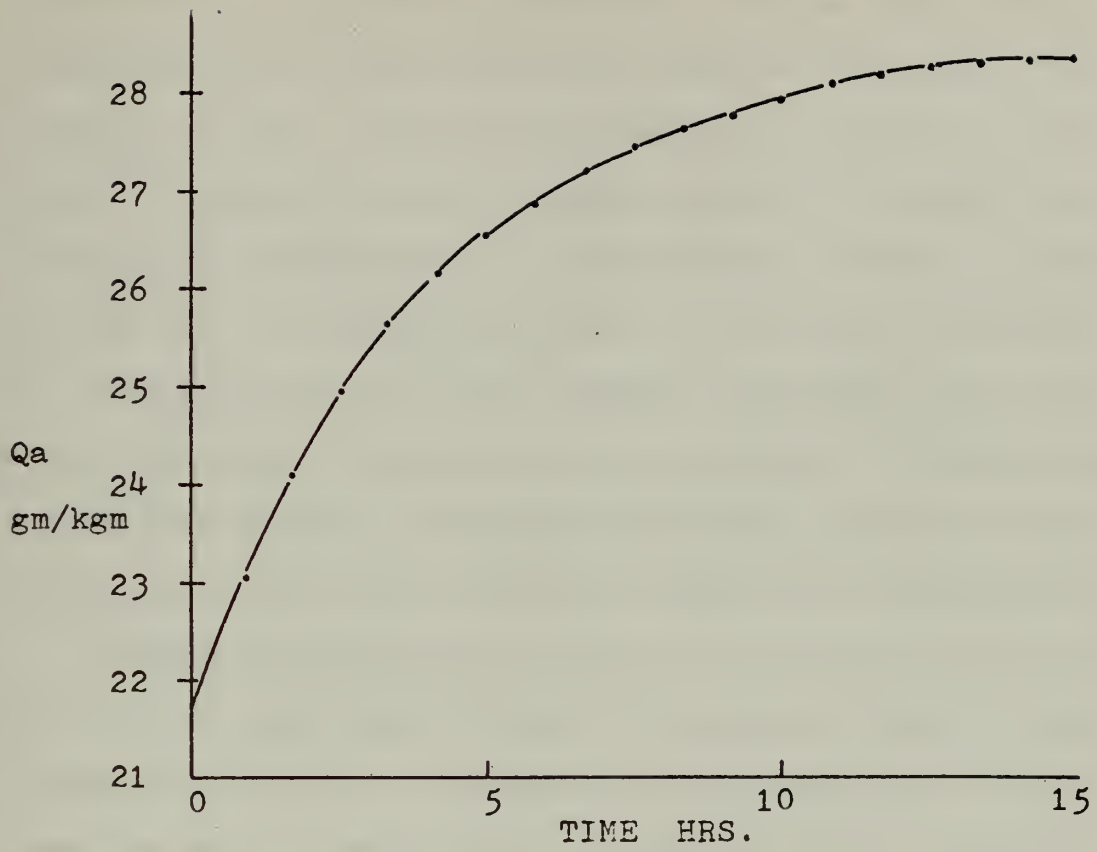

Evolution of specific humidity at the eye wall for the same experiment as described in Fig. 5.

Figure 11

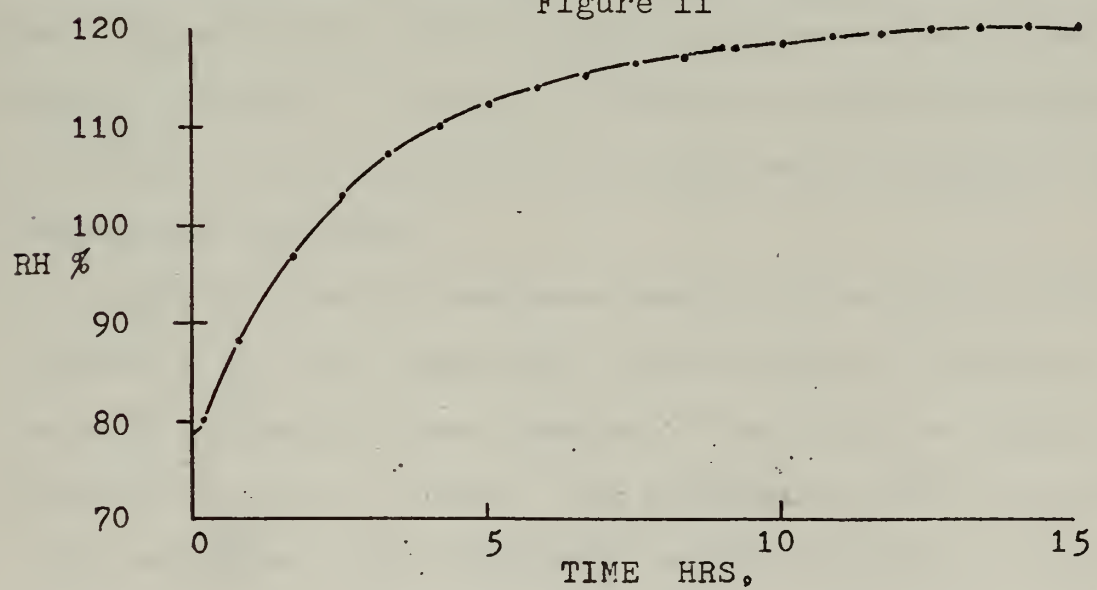

Evolution of relative humidity at the eye wall for the same experiment as described in Fig. 5.

Figure 12

restricted by molecular diffusion. To test this effect, computations were made with the sensible and latent heat exchange in Eqs. (8) and (9) reduced by a factor of one-third. Taking this into account served to decrease the surface air temperature and the moisture content as shown by Fig. 13. It should be noted, if the drag coefficient for momentum had also been reduced, the radial and vertical wind components would have been decreased. A reduced horizontal and vertical transport would have resulted which would have offset the favorable reduction in evaporation.

Another explanation for the accumulation of moisture may be that the model includes no representation of the cumulus clouds or "hot towers" that characterize a hurricane eye wall. Such cumulus convection would transport additional moisture through the top of the boundary layer. Two approaches were used to reduce the excessive accumulation of moisture. The drag coefficient reduction suggested by Robinson was included in all experiments comparing these convective mechanisms.

Convective mechanisms were based upon relative humidity criteria. In each time step, a small amount (initially 0.5 percent) of moisture was removed if the relative humidity exceeded a critical value. The amount of moisture removed could be varied with increasing relative humidity to achieve a balance between the moisture increase due to the horizontal advection and the convective moisture reduction. The amount of moisture removed by this scheme was accumulated and converted to an equivalent depth of precipitation.

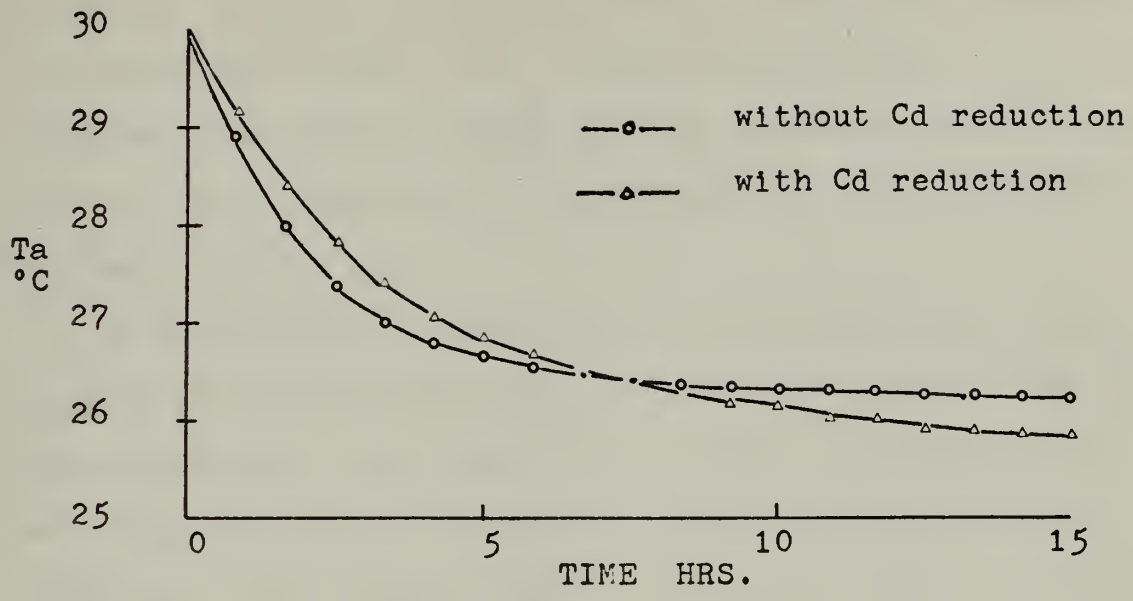

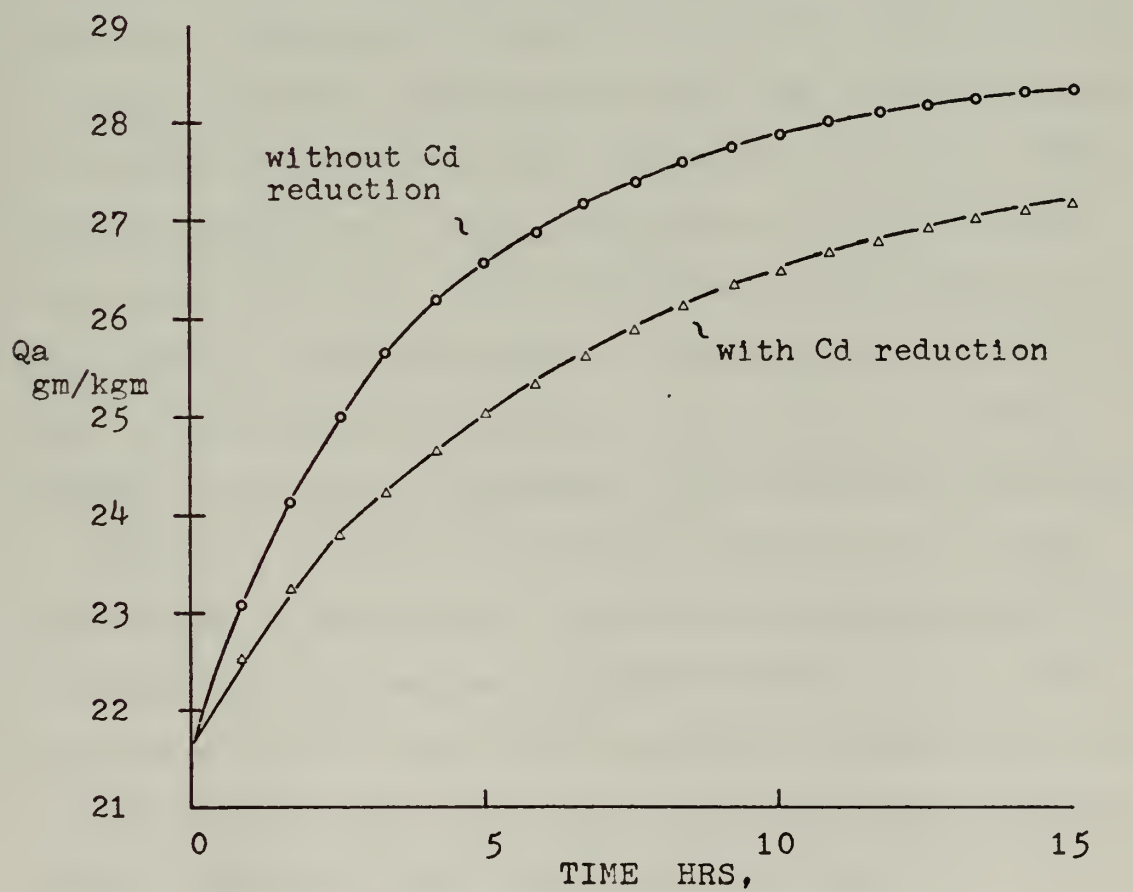

Evolution of atmospheric temperature (upper diagram) and specific humidity (lower diagram) with time for experiment with and without Robinson's C reduction.

Figure 13

The first attempt to simulate cumulus convective mechanism is illustrated in Fig. 14. It was assumed that a convective transfer of moisture through the top of the boundary existed which was just sufficient to maintain the relative humidity at some critical value.

In experiments to establish the critical value for use in this convective mechanism, it was found that the θ_e at the eye wall was very sensitive to small variations. The percentage of specific humidity to be removed was varied along with the relative humidity criterion which initiates the mechanism. Figures 16 and 17 show that variation of either the percentage or relative humidity criterion caused a varying specific humidity content. The specific humidity is crucial in determining the equivalent potential temperature at the eye wall, θ_{ei}, which specifies the maximum wind speed, Eq. (17). Small modification procedures produced rather large variations in the intensity of the hurricane. Therefore specification of the critical relative humidity essentially determined the steady-state hurricane.

The first attempt at moisture reduction led to some improvement in the model. By preventing super-saturation, the moisture field was more representative. One of the objectives of the study was to achieve a steady-state condition in the hurricane when the ocean temperature was held fixed. However it was found that regardless of the initial maximum tangential wind speed, the predicted hurricane had the same intensity, as shown in Fig. 18. For experiments

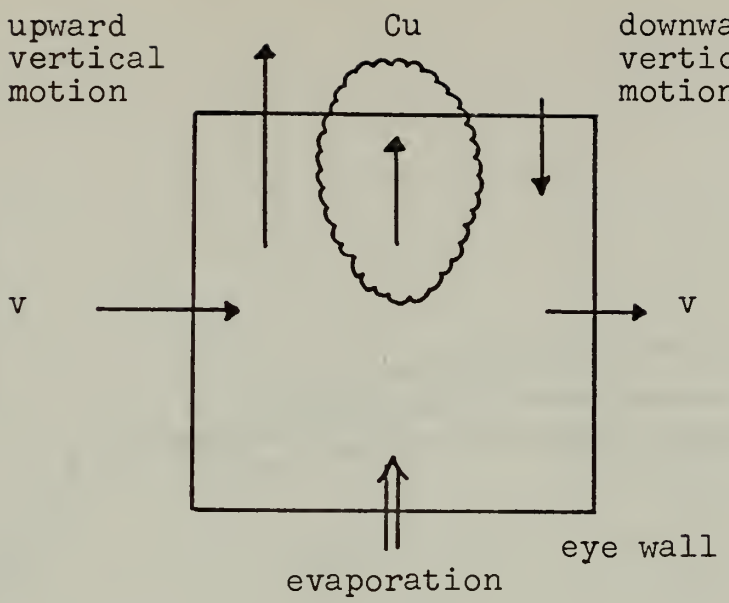

Convective moisture mechanism without Ta adjustment. Note that a loss of moisture through top of boundary layer occurs with ascent in cloud and compensating descent in the environment.

Figure 14

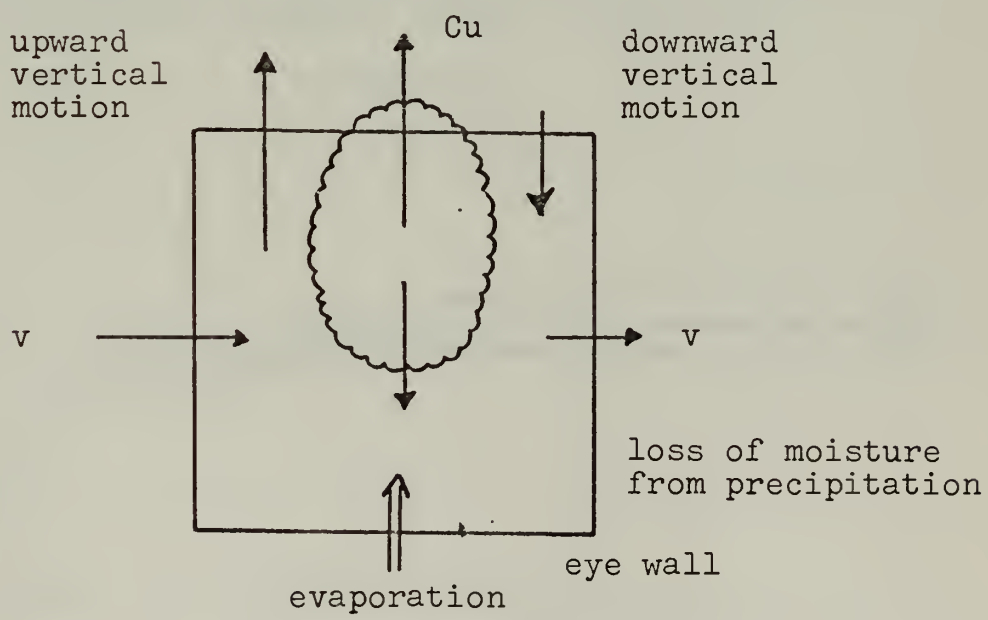

Convective moisture mechanism with Ta adjustment. Note that warming from the release of latent heat occurs in boundary layer.

Figure 15

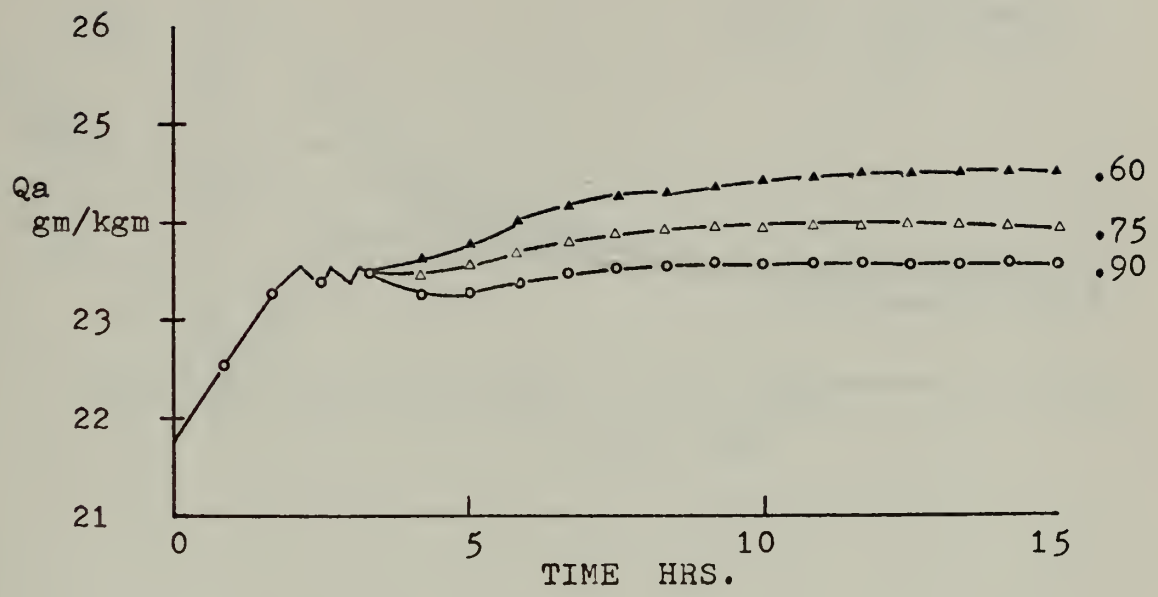

Specific humidity with varying amounts of convective moisture reduction (fraction of 1% removal) for a critical relative humidity of 95%. (See text.)

Figure 16

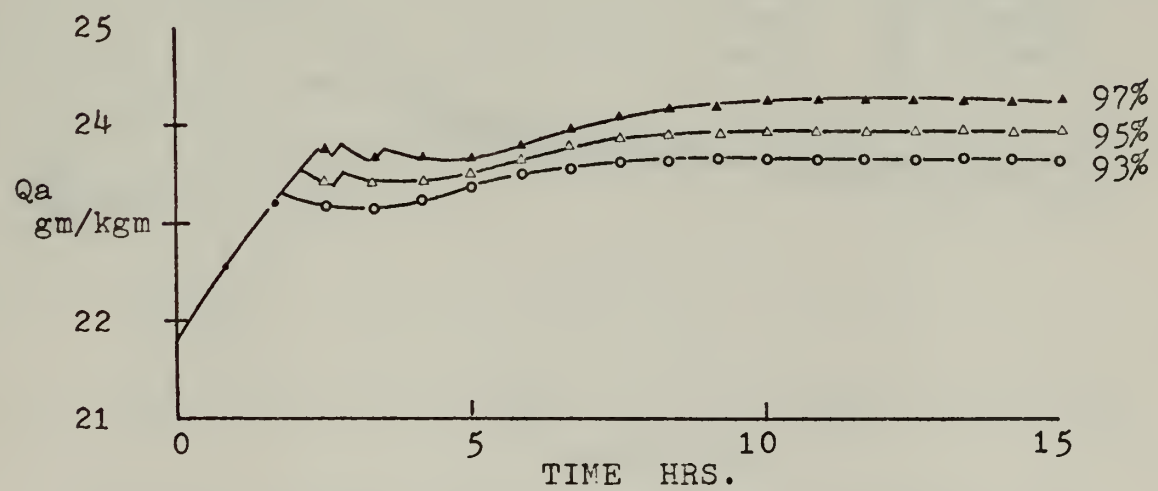

Specific humidity with varying relative humidity criteria for a convective moisture reduction of .75 of 1%. (See text.)

Figure 17

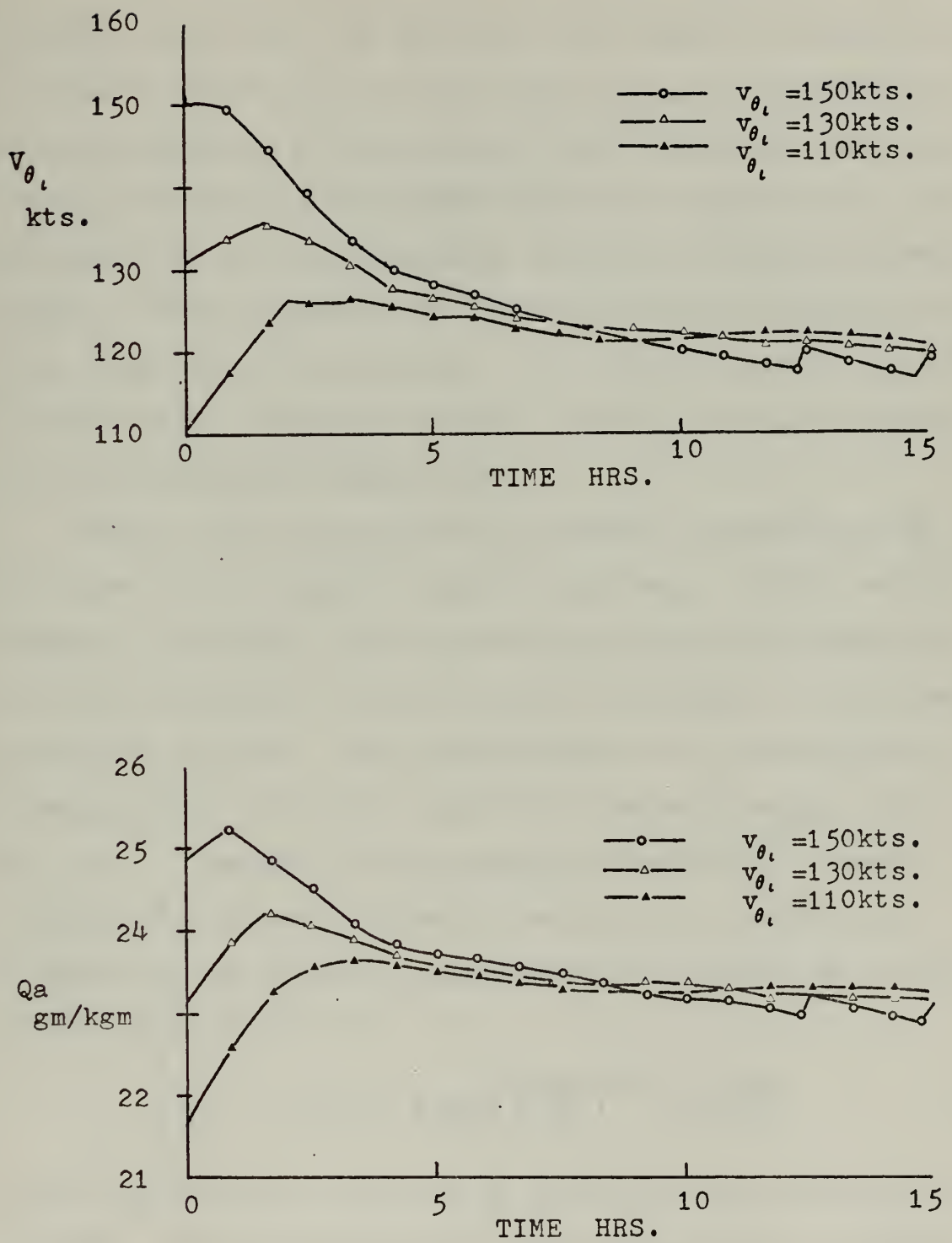

Maximum tangential wind speed (upper diagram) and specific humidity (lower diagram) for various initial v_{θ_i} values with a convective mechanism without a temperature adjustment.

Figure 18

with high initial wind speeds, and thus high specific humidity values near the eye wall, the removal of moisture by increased convection was not offset by an increased potential temperature of the surface air. Therefore there was a steady decrease in equivalent potential temperature at the eye wall, with a corresponding decrease in the wind speed, until a balance between the convective flux of moisture and the evaporation was achieved. This led to a second approach to offset the decreased specific humidity with an increase in the atmospheric temperature.

Recall that the equivalent potential temperature, Θ_e, is conserved in a moist adiabatic process. In the second approach (see Fig. 15), the percentage moisture reduction is still utilized, but the process is assumed to be a psuedo-adiabatic process. This modification was accomplished by computing the equivalent potential temperature, Θ_e, from Eq. (24). The equivalent potential temperature is maintained after the reduction of the specific humidity by increasing the potential temperature of the air to a value given approximately by,

$$T_a = -273.2 + \Theta_e \Big/ \left(\frac{1000}{P}\right)^{.286} e^{\frac{L Q_a}{C_p T_a}} \qquad (25)$$

where the previous value of Ta is used in the denominator. Yet Fig. 19 demonstrates that too much warming accompanied the moisture decrease. The equivalent potential temperature increased slowly, resulting in a corresponding growth in maximum tangential wind speed. Therefore a second

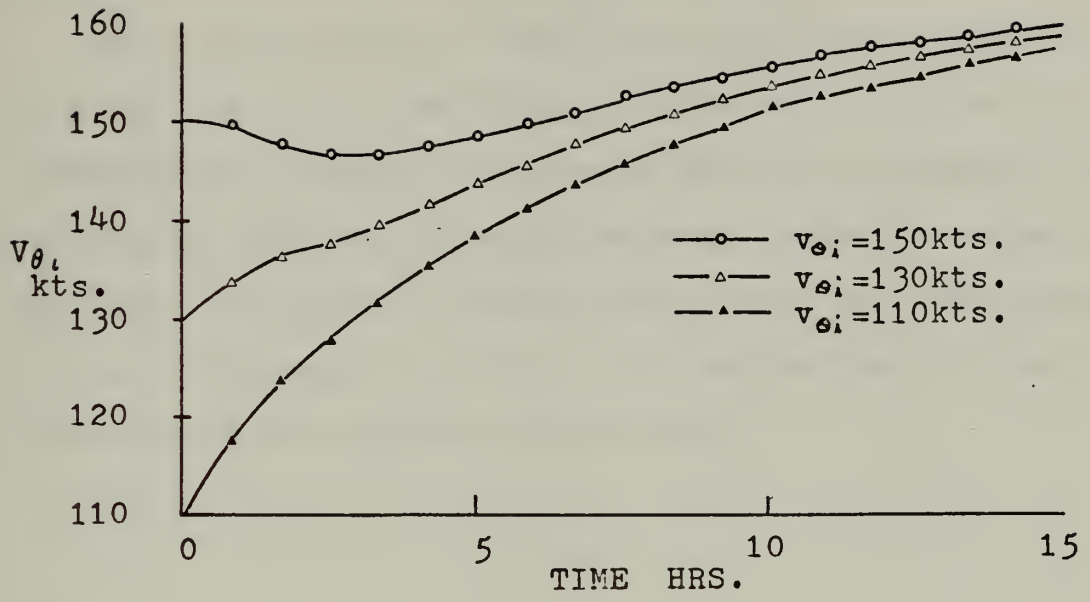

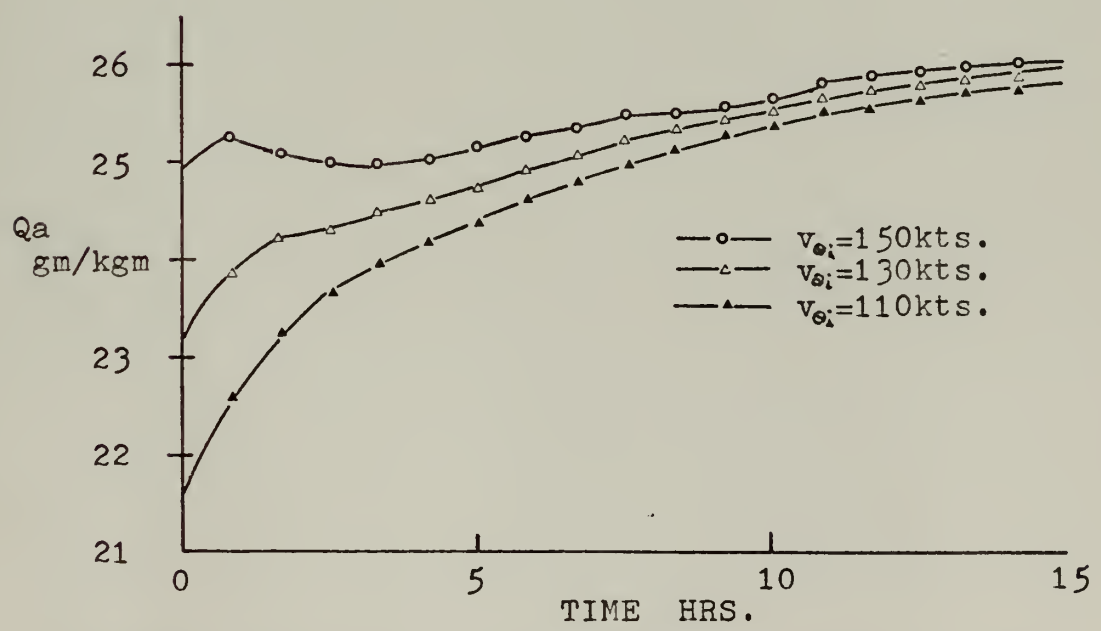

Maximum tangential wind speed (upper diagram) and specific humidity (lower diagram) for various initial v_{θ_i} values with a convective mechanism with a temperature adjustment.

Figure 19

"steady-state hurricane" has been described for a different specification of the convective mechanism.

These experiments to reduce the predicted excess moisture point out the sensitivity of the model. Evidently a combination of moisture transport out of the boundary layer, along with some precipitation warming within the layer, is necessary to produce a steady-state hurricane. Experimentation is necessary to relate the combination of these two effects to the intensity of the storm.

V. OCEAN MODEL PROFILES

Two nearly steady-state models of the atmospheric flow, presented in the modification of the model section, allow comparison of the effect of hurricane circulation upon the ocean profile. The ocean temperature was allowed to vary, due to wind mixing.

A comparison of hurricane heat potential (HHP) and the changes in sea-surface temperature, Tw, will be made to show the effect of the two hurricanes. Hurricane heat potential is a function of the sensible and latent heat transfer as given by Eqs. (8) and (9). The change in this parameter represents the total energy loss experienced by the ocean due to the air-sea boundary fluxes. The greatest loss of heat potential occurred near the eye wall where the latent and sensible heat transfer was the largest, as shown by Figs. 20 and 22. The accumulated energy loss increased with time with a loss of 1600-1900 cal/sq cm per day being accounted for by this approach. This energy loss is small compared to an atmospheric heat balance calculation of Malkus (1962), in which the total energy loss approached 3000 cal/sq cm per day. In the present model the hurricane heat potential calculation does not include radiation, or advection and upwelling effects.

Comparison of Figs. 20 and 22 indicates that the heat potential loss near the eye wall was less for the atmospheric

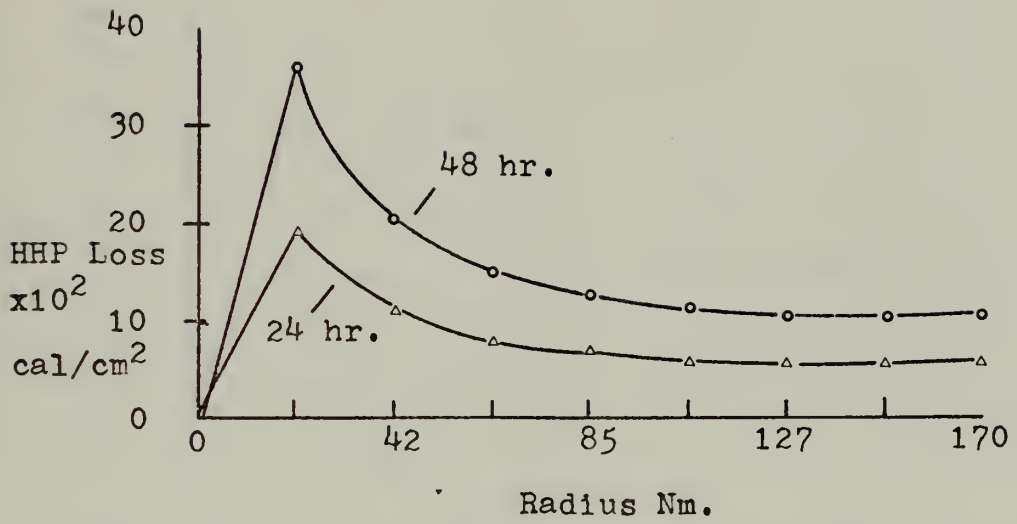

Hurricane heat potential loss for varying daily observations for a convective mechanism without a temperature adjustment.

Figure 20

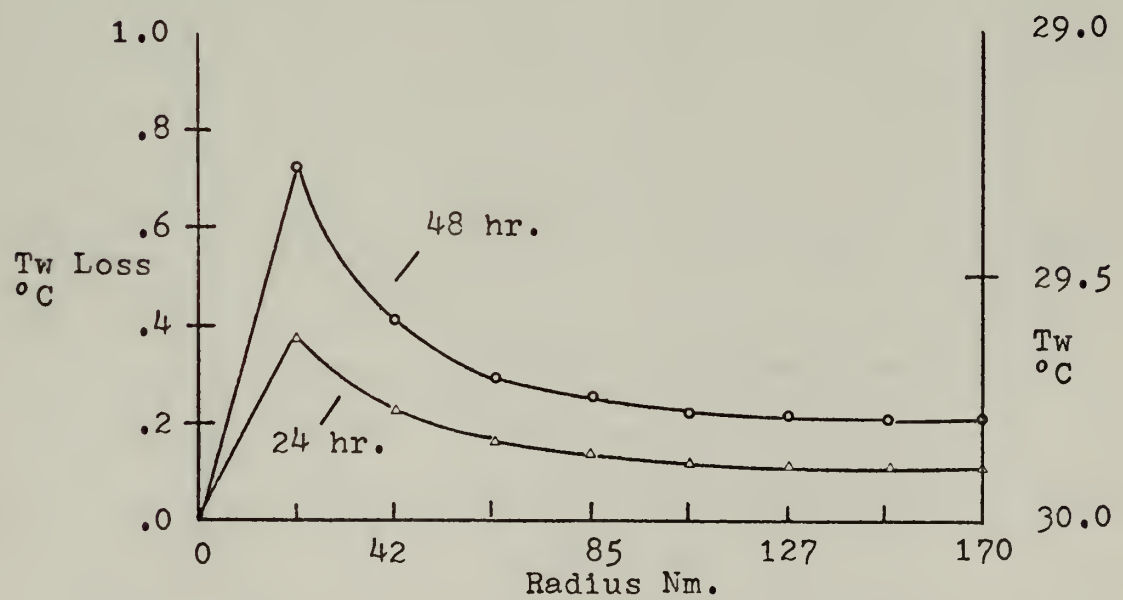

Sea-surface temperature loss for varying daily observations for a convective mechanism without a temperature adjustment.

Figure 21

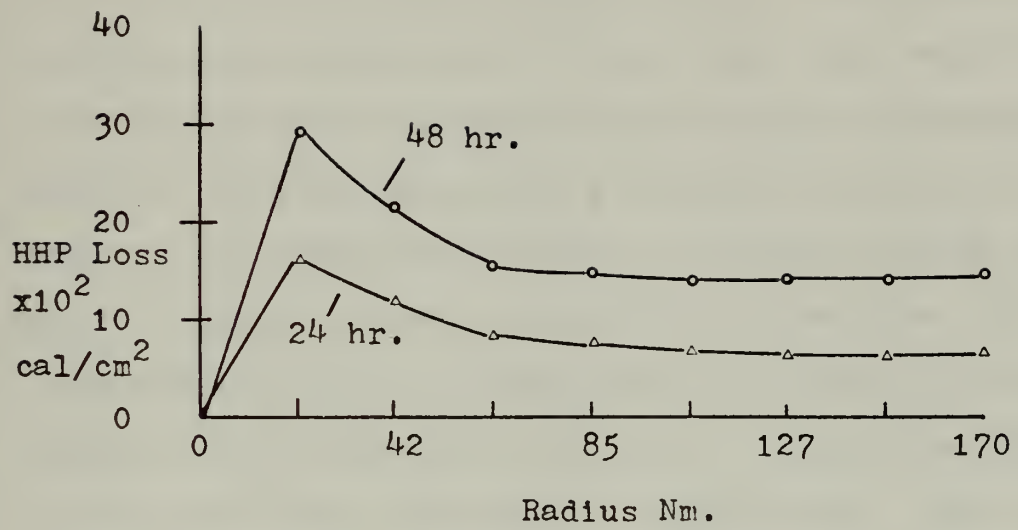

Same as Fig. 20 except for convective mechanism with a temperature adjustment.

Figure 22

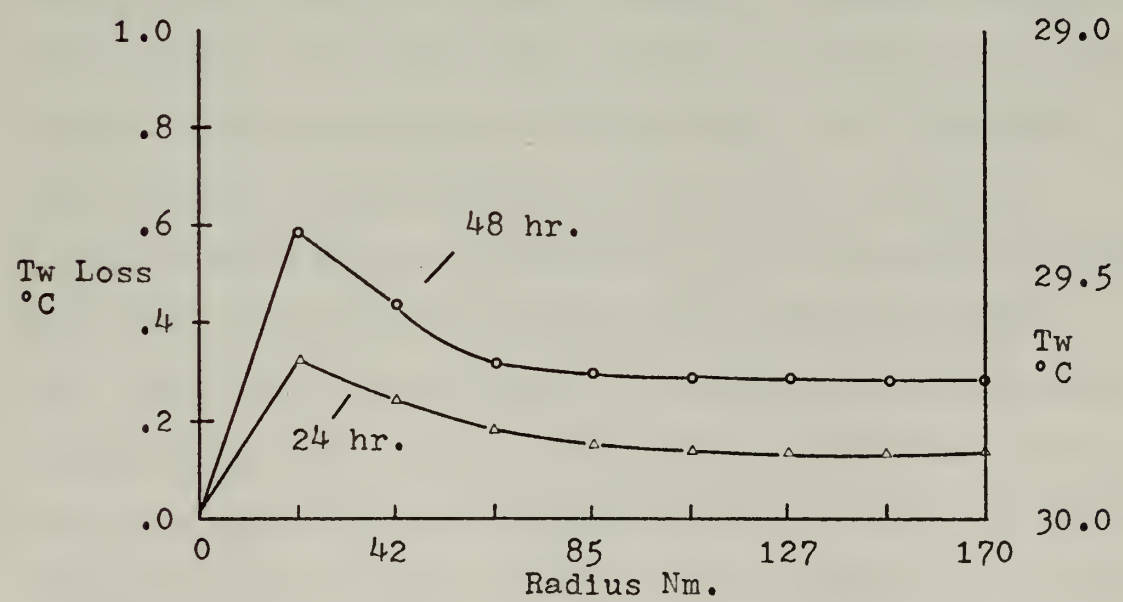

Same as Fig. 21 except for convective mechanism with a temperature adjustment.

Figure 23

model with a convective mechanism with the temperature adjustment. This result was some what surprising since the wind speeds were larger in this model. The sensible and latent heat transfers near the eye wall were smaller because the air-sea temperature and moisture differences were smaller. In this region where convective heating was important, the temperature tends to increase through precipitation warming. As the sea-surface temperature, Tw, decreased and the air temperature, Ta, increased, the sensible heat transfer was smaller. A similar explanation can be given for a reduction in evaporation. That is, the specific humidity, Qa, was larger (for the same critical relative humidity) in the adjusted temperature case because the saturation limit increases with temperature. Away from the eye wall, the wind speed became the dominant factor in the sensible and latent heat transfer equations. As shown in Fig. 22, the change in HHP was larger at these radii for the convective mechanism with temperature adjustment.

The simple model of calculating the sea-surface temperature from the loss of hurricane heat potential (HHP), Eqs. (15) and (16), resulted in a temperature field which cooled with time. Since the cooling occurs over a deep layer a nearly uniform cooling rate of .3 - .4C per day was noted near the eye wall region. This cooling rate is small compared with observed values of 1 - 2C cooling, as might be expected since radiation, horizontal advection in the ocean and upwelling effects have not been included. The resulting

sea-surface temperature fields point out the same features when comparing the two different convective mechanisms as were noted in the hurricane heat potential discussion.

Evolution of the maximum tangential wind speed over an extended period of integration is shown in Fig. 24. As noted previously the maximum tangential wind speed had a lower value without a temperature adjustment than when the surface temperature was adjusted for the effect of precipitation heating within the boundary layer. When the ocean temperature was allowed to vary, the resulting maximum wind speeds were slightly lower even in the first few hours, Fig. 24. As the ocean surface cooled, the sensible heat transfer decreased, and produced slightly cooler atmospheric temperatures at the eye wall. Again, restrictions on the relative humidity value reduced the specific humidity, resulting in a lower tangential wind component.

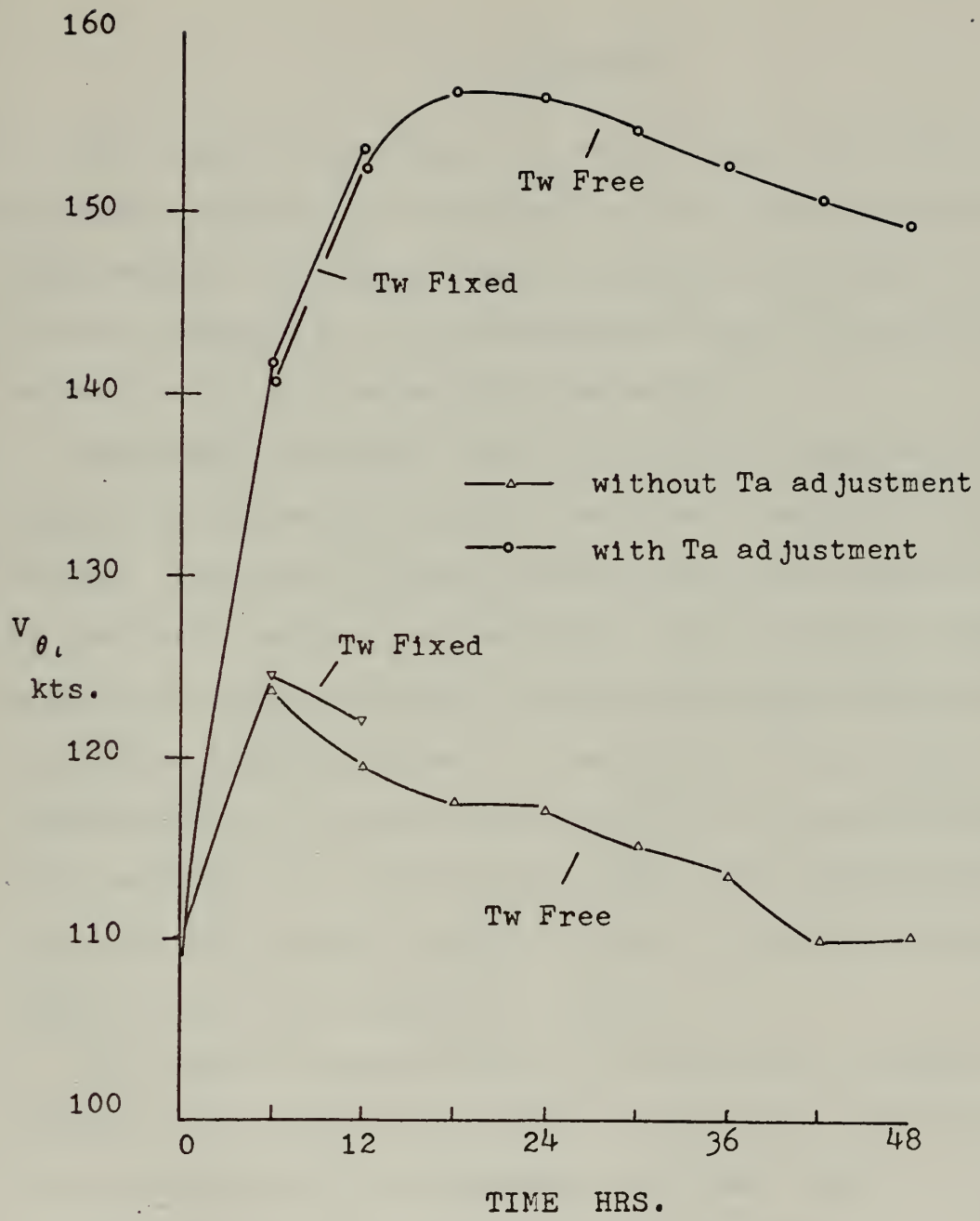

Comparison of maximum tangential wind speed with sea-surface temperature fixed (Tw fixed) and sea-surface temperature allowed to vary (Tw free) for the model incorporating a convective mechanism with and without temperature adjustment.

Figure 24

VI. CONCLUSION

This research utilized the steady-state hurricane model proposed by Riehl in experiments with a simple interacting ocean model. The purpose was to examine the effect of the air-sea exchange in a fixed boundary layer on the hurricane vortex and on the sea-surface temperature.

The model predicted fields of hurricane parameters which compare with observed surface features of mature tropical storms. The radial inflow profile within the boundary layer is realistic, with a corresponding vertical motion field similar to observed values. Because the model does not have a detailed boundary layer, the solution of the radial wind component due to surface stress is not very sophisticated. More resolution in the boundary layer and inclusion of differences in surface roughness would possibly produce a better radial wind component solution.

The simple representation of temperature advection plus sensible heat exchange produced the observed inward decrease in temperature in the atmospheric boundary layer. However an excessive accumulation of moisture occurred in the boundary layer. Two attempts to correct for this situation have shown that small changes in the surface moisture and temperature values strongly affect the maximum wind speed predicted. The proportion of the water vapor transported out of the top of the boundary layer without adding latent

heat to the boundary layer appears to be an important factor in determining the intensity of a steady-state hurricane.

Although the ocean model is quite simple, realistic horizontal oceanic temperature profiles with respect to the hurricane center were obtained. However the magnitude of changes in oceanic heat content and the sea-surface temperatures were smaller than expected in actual hurricanes, since advection and upwelling effects were not included in the ocean model. A steady-state cannot be reached in a stationary storm because of the decreasing sea-surface temperature field. Provision for movement of the hurricane with respect to the ocean would allow prediction of the intensity of the atmospheric system and the oceanic effects. Improvement of the oceanic model, to include a combination of vertical mixing and upwelling, would also give a more realistic view of the consequences of air-sea interaction below a hurricane.

BIBLIOGRAPHY

Fisher, E. L., 1958: Hurricanes and the sea-surface temperature field. J. Meteor., 15, 328-333.

Jordan, C. L., 1964: On the influence of tropical cyclones on the sea surface temperature field. Proc. Symp. Trop. Meteor., New Zealand Meteor. Service, Wellington, 614-622.

Leipper, D. F., 1967: Observed ocean conditions and hurricane Hilda, 1964. J. Atmos. Sci., 24, 182-196.

Leslie, L. M., and R. K. Smith, 1970: The surface boundary layer of a hurricane. II. Tellus, 22, 288-296.

Malkus, J. S., 1962: Large scale interactions. The Sea, Vol. 1, Physical Oceanography, New York, Interscience Publishers, 88-294.

Malkus, J. S. and H. Riehl, 1960: On the Dynamics and Energy Transformations in steady-state Hurricanes. Tellus, 12, 1-20.

O'Brien, James J., and R. O. Reid, 1967: The non-linear response of a two-layer, baroclinic ocean to a stationary, axially-symmetric hurricane: Part I. Upwelling induced by momentum transfer. J. Atmos. Sc., 24, 205-215.

Riehl, H., 1954: Tropical Meteorology. New York, McGraw-Hill Book Co., 281-356.

Riehl, H. and J. S. Malkus, 1961: Some aspects of hurricane "Daisy", 1958. Tellus 13, 181, 213.

Riehl, H., 1963: Some relations between wind and thermal structure of steady-state hurricanes. J. Atmos. Sci., 20, 276-287.

Robinson, G. D., 1966: Another look at some problems of the air-sea interface. Quart. J. R. Met. Soc., 92, 451-465.

Volgenau, D., 1970: Hurricane Heat Potential of the Gulf of Mexico, M. S. Thesis, Naval Postgraduate School, Monterey.

INITIAL DISTRIBUTION LIST

		No. Copies
1.	Defense Documentation Center Cameron Station Alexandria, Virginia 22314	2
2.	Library, Code 0212 Naval Postgraduate School Monterey, California 93940	2
3.	R. L. Elsberry Code 51 Es Naval Postgraduate School Monterey, California 93940	8
4.	Lieutenant L. B. Corgnati, Jr. USS Wasp (CVS-18) FPO New York, New York 09501	2
5.	Department of Meteorology Code 51 Naval Postgraduate School Monterey, California 93940	2
6.	K. L. Davidson Code 51 Ds Naval Postgraduate School Monterey, California 93940	1
7.	Environmental Prediction Research Facility Naval Postgraduate School Monterey, California 93940	1

Security Classification

DOCUMENT CONTROL DATA - R & D

(Security classification of title, body of abstract and indexing annotation must be entered when the overall report is classified)

1. ORIGINATING ACTIVITY (Corporate author)

Naval Postgraduate School
Monterey, California 93940

2a. REPORT SECURITY CLASSIFICATION

Unclassified

2b. GROUP

3 REPORT TITLE

Experiments With A Simple Hurricane-Interacting Ocean Model

4 DESCRIPTIVE NOTES (Type of report and inclusive dates)

Master's Thesis; September 1971

5. AUTHOR(S) (First name, middle initial, last name)

Leino B. Corgnati, Jr.

6. REPORT DATE	7a. TOTAL NO. OF PAGES	7b. NO. OF REFS
September 1971	56	12

8a. CONTRACT OR GRANT NO.	9a. ORIGINATOR'S REPORT NUMBER(S)
b. PROJECT NO.	
c.	9b. OTHER REPORT NO(S) (Any other numbers that may be assigned this report)
d.	

10 DISTRIBUTION STATEMENT

Approved for public release; distributicn unlimited.

11. SUPPLEMENTARY NOTES	12. SPONSORING MILITARY ACTIVITY
	Naval Postgraduate School Monterey, California 93940

13. ABSTRACT

The equations developed by Riehl (1963) for a steady, symmetrical hurricane are used to specify a vortex over a fixed depth boundary layer, which interacts with a simple ocean model. Only vertical mixing in the surface layer is included in the oceanic portion of the model. Interaction of the atmosphere and the ocean occurs through the prediction of boundary layer parameters. Comparison of the predicted boundary parameters with observed mature tropical storms shows good agreement for all variables except the specific humidity, which exceeds saturation. Two attempts to correct for this situation have shown the proportion of the water vapor transported out of the top of the boundary layer without adding latent heat to the boundary layer appears to be an important factor in determining the intensity of a steady-state hurricane.

Although the ocean model is quite simple, realistic horizontal oceanic temperature profiles with respect to the hurricane center were obtained.

DD FORM 1 NOV 65 1473 (PAGE 1)

S/N 0101-807-6811

Security Classification

A-31408

KEY WORDS	LINK A		LINK B		LINK C	
	ROLE	WT	ROLE	WT	ROLE	WT
hurricane						
atmospheric model						
oceanic model						

Thesis 129790
C75465 Corgnati
c.1 Experiments with a
simple hurricane-in-
teracting ocean model.